Selective Area Control of Self-Assembled Pattern Architecture Using a Lithographically Patternable Block Copolymer

Joan K. Bosworth,[†,‡,⊥] Charles T. Black,[§] and Christopher K. Ober[‡,*]

[†]Department of Chemistry and Chemical Biology, Cornell University, Ithaca, New York 14853, [‡]Department of Materials Science and Engineering, Cornell University, Ithaca, New York 14853, and [§]Center for Functional Nanomaterials, Brookhaven National Laboratory, Upton, New York 11973. [⊥]Present address: Hitachi Global Storage Technologies, San Jose, CA 95135.

ABSTRACT We leverage distinctive chemical properties of the diblock copolymer poly(α-methylstyrene)-*block*-poly(4-hydroxystyrene) to create for the first time high-resolution selective-area regions of two different block copolymer phase morphologies. Exposure of thin films of poly(α-methylstyrene)-*block*-poly(4-hydroxystyrene) to nonselective or block-selective solvent vapors results in polymer phase separation and self-assembly of patterns of cylindrical-phase or kinetically trapped spherical-phases, respectively. Poly(4-hydroxystyrene) acts as a high-resolution negative-tone photoresist in the presence of small amounts of a photoacid generator and cross-linker, undergoing radiation-induced cross-linking upon exposure to ultraviolet light or an electron beam. We use lithographic exposure to lock one self-assembled phase morphology in specific sample areas as small as 100 nm in width prior to film exposure to a subsequent solvent vapor to form a second self-assembled morphology in unexposed wafer areas.

KEYWORDS: self-assembly · block copolymer · photoresist · solvent annealing · PαMS-*b*-PHOST

While block copolymer self-assembly holds much promise as a lithography alternative for critical high-resolution patterning of future microelectronic devices,[1] a real limitation of this approach compared to traditional lithography is that self-assembled patterns consist of only a single phase morphology (for example, spheres, cylinders, or lamellae).[2] This is because block copolymer patterns form by phase separation into domain morphologies determined by the constituent polymer block volume fractions, which are constant for a given material.

Here we demonstrate for the first time the ability to selectively pattern the *phase morphology* of a self-assembled block copolymer thin film, an attractive prospect for high-resolution templating applications requiring precise control of the locations of *more than one type* of self-assembled pattern. Our process is enabled by distinctive properties of the block copolymer poly(α-methylstyrene)-*block*-poly(4-hydroxystyrene) (PαMS-*b*-PHOST), which behaves as a chemically amplified negative-tone photoresist when combined with small amounts of a photoacid generator (e.g., triphenylsulfonium triflate, TPST) and a cross-linker (e.g., tetramethoxymethyl glycoluril, TMMGU).[3,4]

We have previously demonstrated control of the self-assembled pattern morphology in PαMS-*b*-PHOST films by exposure to suitable solvent vapor.[5] Exposure of a 33% PαMS polymer film to tetrahydrofuran (THF), a good solvent for both PαMS and PHOST blocks, results in phase separation into a cylindrical film morphology. Annealing in acetone, a solvent selective for the PHOST majority component, causes an order−order transition in the swollen state to spherical morphology, which is kinetically trapped upon drying.

We can use sequential solvent vapor treatments to reversibly switch between PαMS-*b*-PHOST film phase morphologies. However, cross-linked PHOST domains remain fixed and do not change morphology upon exposure to subsequent solvent, allowing the selective formation of regions of two different morphologies within a single PαMS-*b*-PHOST film. A different self-assembling block copolymer system with photoresist behavior, polystyrene-*block*-poly(*tert*-butylacrylate), was shown to behave as a positive-tone photoresist with ~400 nm resolution upon inclusion of a photoacid generator, in which the acid formed upon UV exposure catalyzes deprotection of the poly(*tert*-butyl acrylate) block.[6] The mass loss from block

*Address correspondence to cko3@cornell.edu.

Received for review April 4, 2009 and accepted May 25, 2009.

Published online June 17, 2009.
10.1021/nn900343u CCC: $40.75

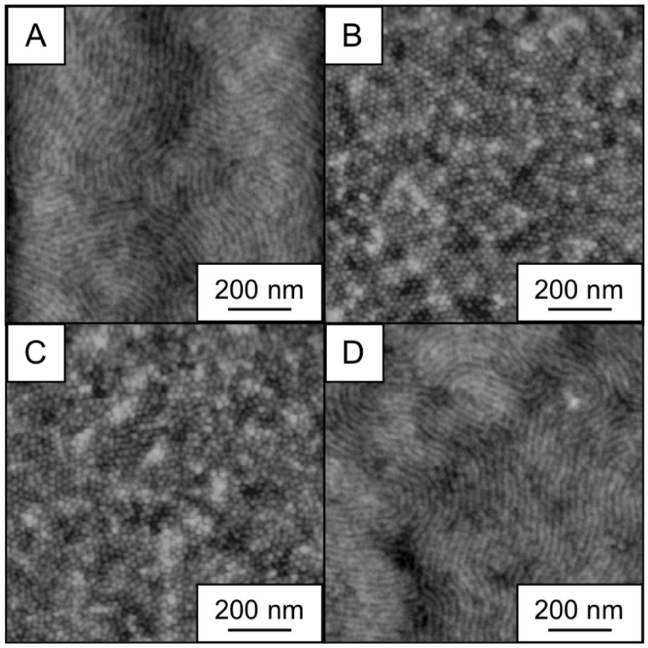

Figure 1. AFM height images of self-assembled PαMS-*b*-PHOST films annealed in different solvent vapor environments: (A) annealed in THF; (B) annealed in acetone; (C) annealed first in THF and then annealed for a second time in acetone; (D) annealed in acetone followed by THF. The height scale for all images is 10 nm.

deprotection can also cause an order−order transition in polymer films, inducing a shift from cylindrical polystyrene-*block*-poly(*tert*-butyl acrylate) to spherical polystyrene-*block*-poly(acrylic acid), although there have been no attempts to achieve multiple phase morphologies in a single polymer film using this approach.[7] Here, we have demonstrated the resolution of our selective-area PαMS-*b*-PHOST patterning approach to be less than 100 nanometers.

Although until now there have been no demonstrations of selective-area patterning of two self-assembled phase morphologies within a single block copolymer film, there have been several demonstrations showing control of two domain *orientations* within a block copolymer film composed of a *single phase morphology*. Surface-neutralizing techniques have been used extensively to gain perpendicular orientation of both cylindrical and lamellar morphologies of polystyrene-*block*-poly(methyl methacrylate) (PS-*b*-PMMA).[8−14] Patternable surface neutralization materials have been demonstrated to form perpendicular orientations on within neutral surface patterns and parallel orientations on untreated areas, although the patterned regions are limited to micrometer-scale resolution.[11−14] Alternatively, chemical epitaxy, in which chemical patterns on a substrate having a length scale similar to the block copolymer can induce alignment in block copolymer film, both by aligning the morphology and controlling the orientation of cylindrical and lamellar domains in films of PS-*b*-PMMA in select wafer areas.[15−19] An advantage to the cross-linking-induced patterning of PαMS-*b*-PHOST demonstrated here is the ability to directly write the high-resolution morphology pattern. Using the selective-cross-linking method demonstrated here, large defect-free patterns can in principle be achieved by combining lithographic exposure with established methods of inducing order in block copolymer films, including not only chemical epitaxy, but also graphopitaxy,[5,20−23] electric fields,[24−27] and shear forces.[28−31]

RESULTS AND DISCUSSION

The key to using PαMS-*b*-PHOST for this combined patterning method is that the presence of the photoacid generator TPST and cross-linker TMMGU (necessary for the material to act as a negative-tone photoresist) do not interfere with the solvent vapor-induced self-assembly processes. Sequential exposure of 20 nm thick PαMS-*b*-PHOST films containing 1.5% w/w TPST and 4% w/w TMMGU to different solvent vapor environments results in self-assembled patterns corresponding to the final solvent vapor treatment (Figure 1). The pattern self-assembly process is not only unaffected by inclusion of small quantities of photoactive compounds, but the solvent anneal history does not play a role in the pattern morphology. PαMS-*b*-PHOST films annealed in nonselective THF form the fingerprint pattern consistent with parallel-oriented cylindrical phase morphology (Figure 1A), while films exposed to acetone vapor (selective for the PHOST block) form spherical-phase patterns of hexagonally arranged dots (Figure 1B). Subsequent exposure of the cylindrical-phase morphology (Figure 1A) to acetone converts the fingerprint pattern to hexagonal dots (Figure 1C) that are indistinguishable from films annealed singly in acetone (Figure 1B). As well, spherical dot patterns are completely converted to cylindrical morphology by further annealing in THF (Figure 1D). We have avoided possible film cross-linking from ambient light exposure by performing all experiments entirely under yellow light conditions.

We can prevent phase-separated PαMS-*b*-PHOST films from switching morphology upon subsequent solvent vapor annealing by inducing a sufficient cross-link density in the film through controlled exposure to ultraviolet (UV) light (Figure 2). In traditional photolithography, film cross-linking further prevents dissolution of the polymer upon developing in a solvent or aqueous base. PαMS-*b*-PHOST films annealed in a first solvent (in the dark) and subsequently exposed to a sufficient dose of UV light and postexposure baked (115 °C, 60 s) before exposure to a second solvent vapor all maintain the phase morphology from their *first anneal*, demonstrating that film cross-linking prevents morphology switching. Films annealed first in acetone before UV exposure and then THF solvent vapor remain locked in a spherical-phase dot pattern (Figure 2A), while films annealed first in THF, cross-linked with UV light, and then exposed to acetone vapor show the cy-

lindrical pattern morphology of the fingerprint pattern (Figure 2B). We observe significant pattern degradation only in films first annealed in THF prior to cross-linking and subsequent acetone exposure (Figure 2B).

We have measured the UV exposure dose required to lock a self-assembled morphology and prevent switching during subsequent exposure to a second solvent vapor; the exposure dose necessary to lock a spherical morphology is shown in Figure 3. Films initially annealed in acetone form a spherical morphology (Figure 1B), and UV exposure of at least 10.4 mJ/cm^2 preserves the hexagonal dot pattern structure upon further annealing in THF (Figure 3D; also the dotted exposure range in Figure 3A), indicating the introduction of sufficient cross-link density to lock the spherical morphology. Films exposed to lower doses show either a complete switch to cylindrical phase (diagonal striped range in Figure 3A) or a mixed cylinder/sphere morphology (Figure 3C; also the gray range in Figure 3A) after a similar second THF treatment.

We can similarly lock a self-assembled cylindrical phase morphology by exposure to sufficient UV light (Figure 4), although this case requires a larger minimum exposure dose (increased from 10.4 mJ/cm^2 to 15.6 mJ/cm^2) necessary to prevent switching to a cylindrical phase upon a second anneal in acetone (Figure 4D; also the diagonal stripe range in Figure 4A). Cylindrical patterns receiving lower UV exposure doses either switch to spherical morphology upon annealing in acetone (the dotted range in Figure 4A) or form a mixed cylinder and sphere pattern (Figure 4C; also the gray range in Figure 4A). Our observations are consistent with PαMS-*b*-PHOST films requiring a higher degree of swelling in acetone (compared to THF) to gain sufficient mobility for pattern formation. Because acetone is a selective solvent for PHOST, the less-soluble PαMS block crosses the swelling threshold for polymer mobility and, thus, self-assembly, at a larger overall swell ratio than in the case of annealing in a nonselective solvent such as THF. We believe that the higher film swelling condition required for pattern formation in acetone interferes with the morphology of the cross-linked film, thereby resulting in a higher exposure dose required to prevent morphology switching (Figure 4A) as well as larger film roughness (Figure 4D,E) for PαMS-*b*-PHOST films annealed in acetone after cross-linking.

We have also measured the PαMS-*b*-PHOST photoresist sensitivity by UV exposure to a range of doses, followed by a postexposure bake and immersion in a solvent developer (1:2 cyclohexanone/isopropanol). The resulting contrast curve shows the normalized remaining film thickness after development *versus* the UV exposure dose (Figure 5). For a negative-tone photoresist material, the sensitivity is defined by the dose at which 50% of original film thickness remains in the UV exposed regions, in this case, ~6 mJ/cm^2, though typically the exposure dose for patterning is chosen between this value and the exposure dose that gives nearly 100% of the original PαMS-*b*-PHOST resist thickness (here approximately 10.4 mJ/cm^2), thereby limiting the line broadening that occurs upon overexposure.[32]

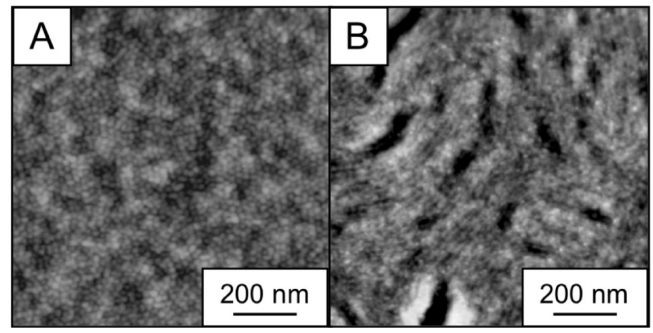

Figure 2. AFM height images of self-assembled PαMS-*b*-PHOST films exposed to UV followed by a postexposure bake prior to the second solvent vapor treatment. (A) A PαMS-*b*-PHOST film annealed in acetone, UV exposed, and annealed in THF remains in a spherical morphology; (B) a film annealed first in THF and exposed to UV, then annealed in acetone maintains the cylindrical morphology of a THF anneal. The height scale for both images is 10 nm.

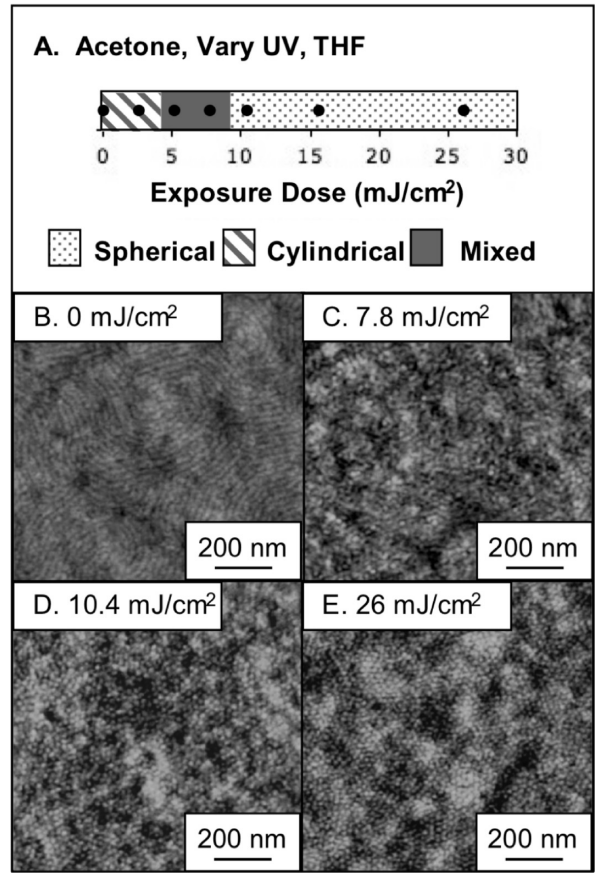

Figure 3. UV exposure dose required to lock the spherical film morphology. (A) UV dose range and resulting block copolymer film morphology after subsequent solvent vapor treatment in THF. The black dots correspond to exposures tested, and the background indicates morphology observed; the interfaces between the morphologies are not known, but for clarity are indicated at the midpoints. AFM height images of PαMS-*b*-PHOST films having UV exposure doses of (B) 0 mJ/cm^2, (C) 7.8 mJ/cm^2, (D) 10.4 mJ/cm^2, and (E) 26 mJ/cm^2. The height scale for (B) is 10 nm, and the scale is 5 nm for (C−E).

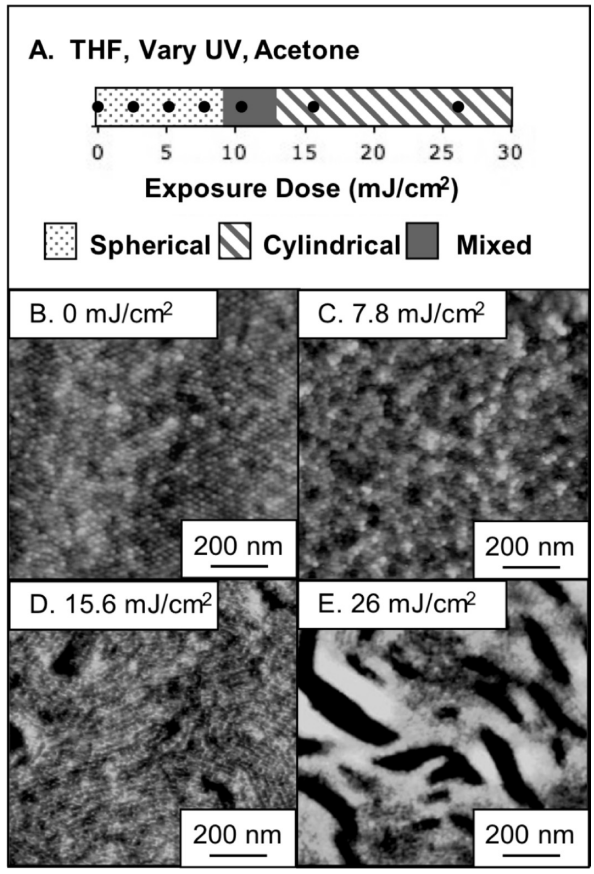

Figure 4. UV exposure dose required to lock the cylindrical film morphology. (A) UV dose range and resulting block copolymer film morphology after subsequent solvent vapor treatment in acetone. AFM height images of PαMS-*b*-PHOST films having UV exposure doses of (B) 0 mJ/cm^2, (C) 7.8 mJ/cm^2, (D) 15.6 mJ/cm^2, and (E) 26 mJ/cm^2. The height scale for images (B−E) is 10 nm.

The required exposure dose to prevent film dissolution (10.4 mJ/cm^2; Figure 5) is the same as the dose to prevent morphology switching in an acetone-to-THF annealing sequence (Figure 3), indicating that the overall resolution for this order of solvent vapor exposures will have a higher resolution than a THF-to-acetone sequence (Figure 4), which has a minimum exposure dose to lock in phase morphology of 15.6 mJ/cm^2.

We combine the UV sensitivity of PαMS-*b*-PHOST together with its solvent vapor processability to form high-resolution patterns of *two different block copolymer phases* within select wafer areas. We have employed electron-beam (e-beam) lithography to investigate the smallest achievable length scales, even though this exposure method requires recalibrating the resist sensitivity for e-beam doses because there is no direct correlation between UV and e-beam sensitivity. We focus on the solvent vapor sequence of first forming a spherical morphology by annealing in acetone and then annealing in THF after e-beam exposure to maximize the patterned film spatial resolution.

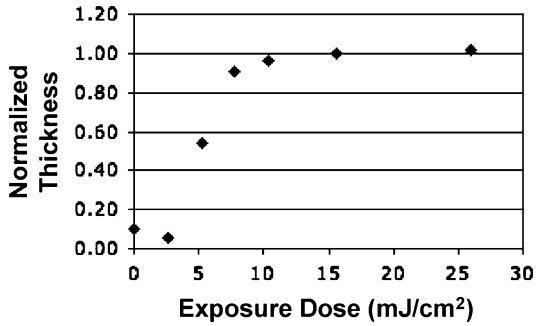

Figure 5. Normalized PαMS-*b*-PHOST film thickness after UV exposure and solvent develop *vs* UV exposure dose.

Film exposure to a range of e-beam doses reveals optimal high-resolution patterns of spherical morphology within a field of cylindrical-phase morphology (Figure 6). PαMS-*b*-PHOST films containing the photoacid generator TPST and the cross-linker TMMGU are annealed first in acetone to form a spherical-phase dot pattern (Figure 1B) and next patterned by e-beam exposure of a series of lines having 1:4 spacing, leading to cross-linking in the exposed regions. The exposed films are next annealed in THF to switch the unexposed regions to a cylindrical morphology. Unlike photolithography, e-beam-exposed PαMS-*b*-PHOST films do not require a postexpose bake prior to solvent annealing, as this was found to increase line broadening. Even without a resist postexpose bake, the optimal exposure dose needed to lock the self-assembled morphology is 5 times smaller for films containing TPST and TMMGU (100 μC/cm^2 for films containing TPST and TMMGU and 500 μC/cm^2 for neat PαMS-*b*-PHOST films, not shown).

PαMS-PHOST films patterned with a 100 μC/cm^2 e-beam exposure dose showed 200 nm wide lines having spherical morphology within a field of cylindrical morphology without significant line broadening (Figure 6A). Written line widths smaller than 200 nm failed to sufficiently cross-link to prevent switching in exposed regions. Unexposed film regions switch to cylindrical morphology during the second solvent vapor treatment, while the exposed regions show a mixed cylinder/sphere morphology, albeit one with minimal line broadening.

Writing a series of 75 nm wide lines with 1:4 spacing using the optimal e-beam dose of 200 μC/cm^2 locks the spherical morphology in regions approximately 4 spheres wide (or ~95 nm, based on the measured 24 nm sphere repeat distance), meaning that this dose produces ~20 nm of line broadening (Figure 6B). We measure a film thickness decrease of ~5 nm in the exposed regions (from an original film thickness of 20 nm) by atomic force microscopy (images not shown).

Higher e-beam exposure doses (Figure 6C) leave the exposed spherical-phase areas unaffected, although we observe a significant increase in line broadening. Overexposure also negatively affects self-assembly of cylindrical phase regions in nominally unexposed areas as cross-links are introduced into these film areas from proximity effects. With lower exposure doses (100 μC/cm^2), we observe virtually no line broadening, but the

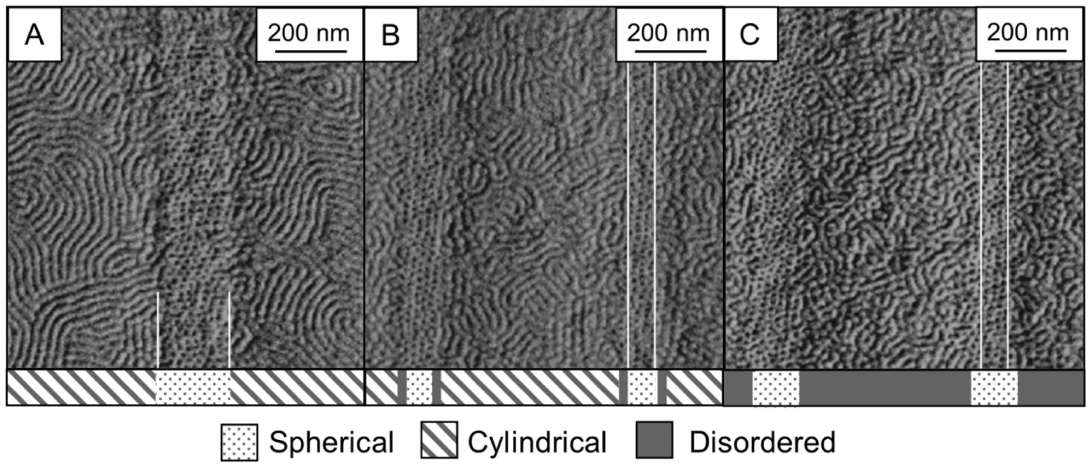

Figure 6. AFM phase images demonstrate a single PαMS-*b*-PHOST film having both regions of spherical morphology and regions of cylindrical morphology. The e-beam exposure doses used are (a) 100 μC/cm², (b) 200 μC/cm², (c) 400 μC/cm². White overlaid lines indicate where e-beam exposed lines were written, and the scale underneath indicates the morphology observed. The phase scale for all images is 6°.

ultimate achievable resolution for the spherical-morphology cross-linked region is worse (Figure 6A, 200 nm lines). The optimum dose is achieved with 200 μC/cm² exposure (Figure 6B): little cross-linking occurs outside of the exposed region and we observe only a narrow band of mixed-phase morphology (less than a single 24 nm domain repeat-unit in width) between exposed and unexposed areas, demonstrating high-resolution and high-contrast patterning of block copolymer film morphologies.

We have demonstrated here that PαMS-*b*-PHOST film morphology can be switched by sequential annealing in solvent vapors having different block selectivities, enabling formation of either spherical or cylindrical morphologies. We can prevent morphology switching in select wafer regions by selective radiation-induced cross-linking using either UV light or an e-beam prior to film exposure to a second solvent vapor environment. By combining e-beam-induced cross-linking and solvent-induced morphology switching, we have shown for the first time selective high-resolution patterning of a single block copolymer film into ~100 nm regions of two different self-assembled phase morphologies.

METHODS

The PαMS-*b*-PHOST block copolymer material used here has a total M_n of 21 kg/mol, 33% PαMS by mass, and distribution 1.10, as described previously;[5] synthesis by sequential anionic polymerization of poly(α-methylstyrene)-*block*-poly(*tert*-butoxystyrene) and subsequent deprotection to PαMS-*b*-PHOST have also been described previously.[3] Films were spin-coated from propylene glycol methyl ether acetate (Aldrich, 1% w/v) with spin speed previously determined to yield single morphology thickness films, measured here to be 20 nm by ellipsometry.[5] Spinning solution also contained 1.5% (w/w relative to PαMS-*b*-PHOST) triphenylsulfonium triflate (TPST, Aldrich) photoacid generator and 4% (w/w relative to PαMS-*b*-PHOST) tetramethoxymethyl glycoluril (TMMGU, "Powderlink 1174," Cytec Industries) cross-linker. These small quantities of TPST and TMMGU do not to affect the self-assembly of the PαMS-*b*-PHOST, as long as films are not exposed.

Spin coating and solvent vapor annealing with acetone (Aldrich) and tetrahydrofuran (THF, Aldrich; in a sealed 1 L jar with solvent reservoir, 6 mL of THF or 4 mL of acetone) are performed under yellow light conditions to prevent photoacid generator exposure. Atomic force microscopy (AFM) is performed on a Veeco Dimension 3100 in tapping mode. In Figure 6, partial removal of the PαMS was achieved by heating films on a hot plate at 115 °C for 15 min in air, aiding AFM imaging.

In the case of UV-exposed films, an HTG mask aligner with 254 nm exposure was used to blanket-expose films; output was measured to be 2.6 mW/cm². Post-exposure bake in all cases was 115 °C for 60 s. Solvent development conditions determined previously[3] were used again here, involving 1:2 cyclohexanone/isopropanol (v/v) mixture for 1 min, followed by 1 min in isopropanol, and dry nitrogen. Electron beam lithography was written using an NPGS on a Helios Nanolab (FEI), with exposures at 30 kV. Films used for e-beam patterning contain TPST and TMMGU, but no postexpose bake step is applied after e-beam patterning. Film thicknesses were measured with a Nanofilm EP3 imaging ellipsometer.

Acknowledgment. This work was supported by the National Science Foundation Materials World Network (Award DMR 0602821), the NSF NIRT (Award CTS 0304159), and the Semiconductor Research Consortium, and J.K.B. was supported by fellowships from Motorola and IBM. Research was carried out in part at the Center for Functional Nanomaterials (CFN) at Brookhaven National Laboratory, which is supported by the U.S. Department of Energy, Division of Materials Sciences and Division of Chemical Sciences, under Contract No. DE-AC02-98CH10886. This work was also performed using facilities at the Cornell NanoScale Facility, (CNF), the Cornell Center for Materials Research (CCMR), and the Cornell Nanobiotechnology Center (NBTC). CNF is a member of the NNIN, supported by NSF Award ECS-0335765, CCMR is supported by NSF Award DMR 0520404, part of the NSF MRSEC program, and the NBTC is supported by the STC Program of the NSF, Award ECS-9876771. The authors thank A. Stein of the CFN as well as D. Forman and J. Sha of Cornell for assistance with e-beam patterning.

REFERENCES AND NOTES

1. Black, C. T. Polymer Self-Assembly as a Novel Extension to Optical Lithography. *ACS Nano* **2007**, *1*, 147–150.
2. Bates, F. S.; Fredrickson, G. H. Block Copolymers - Designer Soft Materials. *Phys. Today* **1999**, *52* (February), 32–38.

3. Li, M.; Douki, K.; Goto, K.; Li, X.; Coenjarts, C.; Smilgies, D.-M.; Ober, C. K. Spatially Controlled Fabrication of Nanoporous Clock Copolymers. *Chem. Mater.* **2004**, *16*, 3800–3808.
4. Du, P.; Li, M.; Douki, K.; Li, X.; Garcia, C. B. W.; Jain, A.; Smilgies, D.-M.; Fetters, L. J.; Gruner, S. M.; Wiesner, U.; Ober, C. K. Additive-Driven Phase-Selective Chemistry in Block Copolymer Thin Films: The Convergence of Top-Down and Bottom-Up Approaches. *Adv. Mater.* **2004**, *16*, 953–957.
5. Bosworth, J. K.; Paik, M. Y.; Ruiz, R.; Schwartz, E. L.; Huang, J. Q.; Ko, A. W.; Smilgies, D.-M.; Black, C. T.; Ober, C. K. Control of Self-Assembly of Lithographically Patternable Block Copolymer Films. *ACS Nano* **2008**, *2*, 1396–1402.
6. La, Y.-H.; In, I.; Park, S.-M.; Meagley, R. P.; Leolukman, M.; Gopalan, P.; Nealey, P. F. Pixelated Chemically Amplified Resists: Investigation of Material Structure in the Spatial Distribution of Photoacids and Line Edge Roughness. *J. Vac. Sci. Technol., B* **2007**, *25*, 2508–2513.
7. La, Y.-H.; Edwards, E. W.; Park, S. M.; Nealey, P. F. Directed Assembly of Cylinder-Forming Block Copolymer Films and Thermochemically Induced Cylinder to Sphere Transition: A Heirarchical Route to Linear Arrays of Nanodots. *Nano Lett.* **2005**, *5*, 1379–1384.
8. Mansky, P.; Liu, Y.; Huang, E.; Russell, T. P.; Hawker, C. Controlling Polymer−Surface Interactions With Random Copolymer Brushes. *Science* **1997**, *275*, 1458–1460.
9. Mansky, P.; Russell, T. P.; Hawker, C. J.; Pitsikalis, M.; Mays, J. Ordered Diblock Copolymer Films on Random Copolymer Brushes. *Macromolecules* **1997**, *30*, 6810–6813.
10. Huang, E.; Pruzinsky, S.; Russell, T. P.; Mays, J.; Hawker, C. J. Neutrality Conditions for Block Copolymer Systems on Random Copolymer Brush Surfaces. *Macromolecules* **1999**, *32*, 5299–5303.
11. Ryu, D. Y.; Shin, K.; Drockenmuller, E.; Hawker, C. J.; Russell, T. P. A Generalized Approach to the Modification of Solid Surfaces. *Science* **2005**, *308*, 236–239.
12. Bang, J.; Bae, J.; Loewenhielm, P.; Spiessberger, C.; Given-Beck, S. A.; Russell, T. P.; Hawker, C. J. Facile Routes to Patterned Surface Neutralization Layers for Block Copolymer lithogrpahy. *Adv. Mater.* **2007**, *19*, 4552–4557.
13. Han, E.; In, I.; Park, S.-M.; La, Y.-H.; Wang, Y.; Nealey, P. F.; Gopalan, P. Photopatternable Imaging Layers for Controlling Block Copolymer Microdomain Orientation. *Adv. Mater.* **2007**, *19*, 4448–4452.
14. Han, E.; Stuen, K. O.; La, Y.-H.; Nealey, P. F.; Gopalan, P. Effect of Composition of Substrate-Modifying Random Copolymers on the Orientation of Symmetric and Asymmetric Diblock Copolymer Domains. *Macromolecules* **2008**, *41*, 9090–9097.
15. Stoykovich, M. P.; Mueller, M.; Kim, S. O.; Solak, H. H.; Edwards, E. W.; de Pablo, J. J.; Nealey, P. F. Directed Assembly of Block Copolymer Blends Into Nonregular Device-Oriented Structures. *Science* **2005**, *308*, 1442–1446.
16. Kim, S. O.; Kim, B. H.; Meng, D.; Shin, D. O.; Koo, C. M.; Solak, H. H.; Wang, Q. W. Novel Complex Nanostructure From Directed Assembly of Block Copolymers on Incommensurate Surface Patterns. *Adv. Mater.* **2007**, *19*, 3271–3275.
17. Park, S.-M.; Craig, G. S. W.; Liu, C.-C.; La, Y.-H.; Ferrier, N. J.; Nealey, P. F. Characterization of Cylinder-Forming Block Copolymers Directed to Assemble on Spotted Chemical Patterns. *Macromolecules* **2008**, *41*, 9118–9123.
18. Cheng, J. Y.; Rettner, C. T.; Sanders, D. P.; Kim, H.-C.; Hinsberg, W. D. Dense Self-Assembly on Sparse Chemical Patterns: Rectifying and Multiplying Lithographic Patterns Using Block Copolymers. *Adv. Mater.* **2008**, *20*, 3155–3158.
19. Ruiz, R.; Kang, H.; Detcheverry, F. A.; Dobisz, E.; Kercher, D. S.; Albrecht, T. R.; de Pablo, J. J.; Nealey, P. F. Density Multiplication and Improved Lithography by Directed Block Copolymer Assembly. *Science* **2008**, *321*, 936–939.
20. Segalman, R. A.; Yokoyama, H.; Kramer, E. J. Graphoepitaxy of Spherical Domain Block Copolymer Films. *Adv. Mater.* **2001**, *13*, 1152–1155.
21. Cheng, J. Y.; Ross, C. A.; Smith, H.; Thomas, E. L. Templated Self-Assembly of Block Copolymers: Top-Down Helps Bottom-Up. *Adv. Mater.* **2006**, *18*, 2505–2521.
22. Black, C. T. Self-Aligned Self Assembly of Multi-Nanowire Silicon Field Effect Transistors. *Appl. Phys. Lett.* **2005**, *87*, 163116.
23. Park, S.; Kim, B.; Yavuzcetin, O.; Tuominen, M. T.; Russell, T. P. Ordering of PS-P4 VP on Patterned Silicon Substrates. *ACS Nano* **2008**, *2*, 1363–1370.
24. Amundson, K.; Helfand, E.; Quan, X.; Hudson, S. D.; Smith, S. D. Alignment of Lamellar Block Copolymer Microstructures in an Electric Field. 2. Mechanisms of Alignment. *Macromolecules* **1994**, *27*, 6559–6570.
25. Xu, T.; Zhu, Y.; Gido, S. P.; Russell, T. P. Electric Field Alignment of Symmetric Diblock Copolymer Thin Films. *Macromolecules* **2004**, *37*, 2625–2629.
26. Boeker, A.; Elbs, H.; Haensel, H.; Knoll, A.; Ludwigs, S.; Zettl, H.; Zvelindovsky, A. V.; Sevink, G. J. A.; Urban, V.; Abetz, V.; Mueller, A. H. E.; Krausch, G. Electric Field Induced Aligment of Concentrated Block Copolymer Solutions. *Macromolecules* **2003**, *36*, 8078–8087.
27. Olszowka, V.; Kuntermann, V.; Boeker, A. Control of Orientational Order in Block Copolymer Thin Films by Electric Fields: A Combinatorial Approach. *Macromolecules* **2008**, *41*, 5155–5518.
28. Chen, Z.-R.; Kornfield, J. A.; Smith, S. D.; Grothaus, J. T.; Satkowski, M. M. Pathways to Macroscale Order in Nanostructured Block Copolymers. *Science* **1997**, *277*, 1248–1253.
29. Angelescu, D. E.; Waller, J. H.; Adamson, D. H.; Deshpande, P.; Chou, S. Y.; Register, R. A.; Chaikin, P. M. Macroscopic Orientation of Block Copolymer Cylinders in Single-Layer Films by Shearing. *Adv. Mater.* **2004**, *16*, 1736–1740.
30. Hamley, I. W. The Effect of Shear on Ordered Block Copolymer Solutions. *Curr. Opin. Colloid Interface Sci.* **2000**, *5*, 341–349.
31. Sebastian, J. M.; Lai, C.; Graessley, W. W.; Register, R. A. Steady-Shear Rheology of Block Copolymer Melts and Concentrated Solutions: Disordering Stress in Body-Centered-Cubic Systems. *Macromolecules* **2002**, *35*, 2707–2713.
32. Ito, H. Chemical Amplification Resists for Microlithography. *Adv. Polym. Sci.* **2005**, *172*, 37–245.